Investigation of High-Temperature Bright Plasma X-ray Sources Produced in 5-MA X-Pinch Experiments

D. B. Sinars,[1] R. D. McBride,[1] S. A. Pikuz,[2] T. A. Shelkovenko,[2] D. F. Wenger,[1] M. E. Cuneo,[1] E. P. Yu,[1] J. P. Chittenden,[3] E. C. Harding,[1] S. B. Hansen,[1] B. P. Peyton,[1] D. J. Ampleford,[1] and C. A. Jennings[1]

[1]*Sandia National Laboratories, P.O. Box 5800, Albuquerque, New Mexico 87185, USA*
[2]*Laboratory of Plasma Studies, Cornell University, Ithaca, New York 14853, USA*
[3]*Blackett Laboratory, Imperial College, London SW7 2BW, United Kingdom*

(Received 28 July 2012; published 9 October 2012)

Using solid, machined X-pinch targets driven by currents rising from 0 to 5–6 MA in 60 ns, we observed bright spots of 5–9-keV continuum radiation from 5 ± 2-μm diameter regions. The >6-keV radiation is emitted in about 0.4 ns, and the bright spots are roughly 75 times brighter than the bright spots measured at 1 MA. A total x-ray power of 10 TW peak and yields of 165 ± 20 kJ were emitted from a 3-mm height. The 3–5-keV continuum radiation had a 50–90-GW peak power and 0.15–0.35-kJ yield. The continuum is plausibly from a 1275 ± 75-eV blackbody or alternatively from a 3500 ± 500-eV bremsstrahlung source.

DOI: 10.1103/PhysRevLett.109.155002 PACS numbers: 52.58.Lq, 52.35.Py, 52.80.Qj

A cylindrical current-carrying plasma can have an inward magnetic pressure from the $\vec{j} \times \vec{B}$ force exceeding its plasma pressure so that it implodes radially, or "pinches." Pinch plasmas frequently produce very brief but intense soft-x-ray bursts from tiny regions that are variously called "bright spots" or "micropinches." Bright spots have been observed in >100-kA single-wire explosions [1], two-wire 200-kA X-pinch plasmas [2], vacuum sparks [3], plasma focus [4,5], and wire-array z pinches [6]. A method for reliably creating a bright spot at a predetermined location to enable it to be studied is an X-pinch configuration [7], in which two or more fine wires are arranged so that they cross at a single point. Experiments with X pinches driven by a 0.2-MA 60-ns linearly rising current found that micropinch plasmas can have sizes of 0.8–1.5-μm diameters [8,9], temperatures of about 1 keV, densities >10% of solid density, and durations of 10–100 ps [2,10,11]. These high-energy density plasmas have a plasma pressure of about 0.4 Gbar, comparable to the 1-Gbar magnetic pressure of 0.2 MA at 1 μm.

Understanding micropinch plasmas is important. For example, 16-MA tungsten wire-array z-pinch experiments contain numerous small, brightly emitting regions in 6.15 keV emission, which may emit about 30% of the total 1-MJ 0.1–10-keV radiation yield [12], including most of the >2-keV radiation. Data from 0.2-MA X-pinch experiments have been explained using a model based on approximate Bennett equilibrium conditions, in which a balance was achieved between blackbody radiation losses and Joule (thermal) heating by the current [13]. Assuming that the collapse ends at a radius of 1 μm, this equilibrium model predicts a ten-times solid-density, 156-Gbar plasma at 1 MA. Recent experiments studying multiwire X-pinch loads at currents of up to 2.3 MA reported spot-size measurements down to about 20 μm, and measured radiation powers of 120 GW in 1–3-keV radiation [14,15]; however, testing the predictions of Ref. [13] requires more detailed data.

Here, we summarize the results obtained from 31 X-pinch experiments conducted on SATURN, a 6-MA, 60-ns pulsed power facility. In which we directly measured several key bright spot parameters for the first time for currents up to 5 MA. The SATURN experiments extend prior work on the 1-MA, 100-ns COBRA facility [16]. We fielded several X-pinch load designs that were first evaluated on 1-MA experiments, including large wire-number cylindrical wire arrays twisted into an X pinch [16], nested multilayered wire arrays twisted into an X pinch [17], and a hybrid configuration in which a single wire is strung across two conical electrodes [16,18,19]. However, most of our SATURN experiments used X-pinch loads with solid, machined cross points, as shown in Fig. 1. The targets were made of tungsten, a W-Cu alloy (47.1–52.9 atomic %), or a Cu-Ni-Mn alloy (53–45.9-1.1 atomic %), with minimum mass per unit length values in the 12–24 mg/cm range. These masses were chosen on the basis of the self-similar implosion scaling law [20], $\Pi = (\mu_0 I^2 \tau^2)/(4\pi m_l r^2)$, where Π is a scaling constant, I is the peak current, τ is the implosion time, m_l is the liner mass per unit length, and r is the radius. Increasing the radius is the only way to vary m_l for solid-density on-axis matter, so that m_l scales linearly with the current. Previous experiments at 1 MA were about 3 mg/cm [16].

Sample current and radiation traces are plotted in Fig. 2. The current in these experiments was measured using B-dot probes located upstream of the load [21]. The first significant >3-keV x-ray burst typically occurred at current values in the range 3–5 MA. As described previously [16], the total soft-x-ray power was measured using x-ray diodes normalized to Ni bolometers and photoconducting

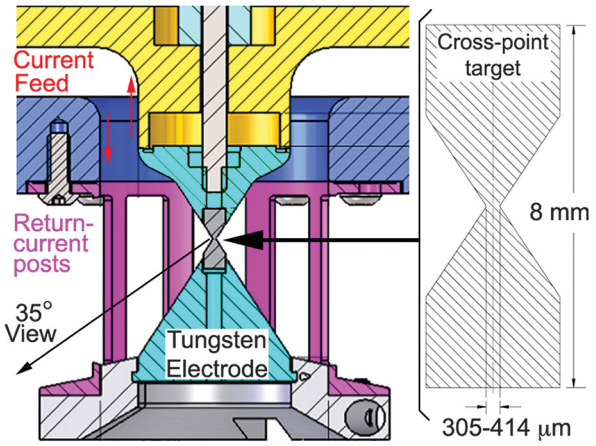

FIG. 1 (color). Half-section drawing of hardware. A solid, machined cross point of the desired material is inserted between two tungsten electrodes as the load of the SATURN facility. Most diagnostics had a 35° view below the horizontal.

diodes (PCDs) filtered with 25-μm Be or 12-μm Ti, measured at >1-keV and 3–5-keV continuum radiation, respectively. The typical peak radiation powers were about 10 TW (total emission), 200–500 GW (> 1 keV), and 15–90 GW (3–5 keV), and the typical x-ray yields were 100–150 kJ (total), 1–5 kJ (> 1 keV), and 50–300 J (3–5 keV). The best radiating material was tungsten, which had a total x-ray peak power of 10 TW and yield of 165 ± 20 kJ, with 3–5 keV radiation peak power of 50–90 GW and yield of 150–350 J.

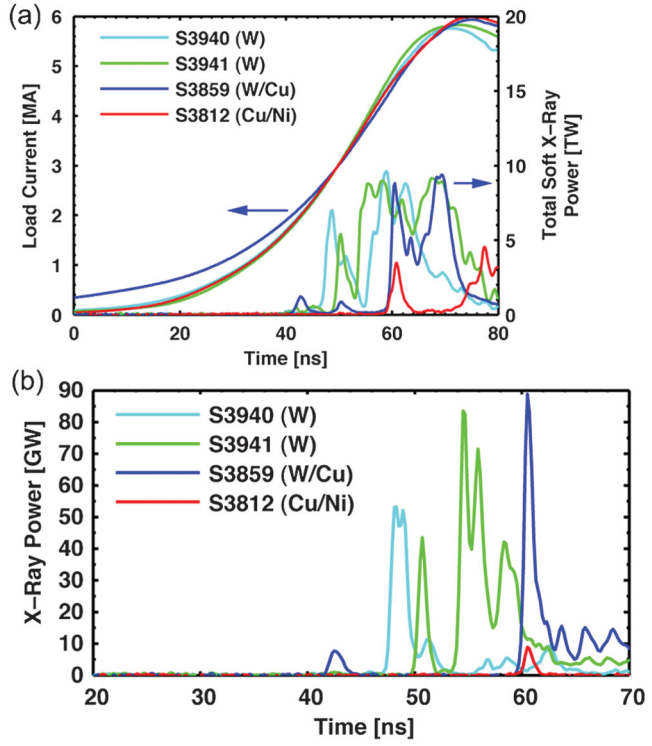

FIG. 2 (color). Sample data from selected X-pinch tests. (a) Total load current and the total soft-x-ray power. (b) 3-5-keV x-ray power measured using a PCD with a 12.5-μm Ti filter.

The diodes were sampled every 200 ps, but this could lead to underestimates of the power for source durations <100 ps. On a limited number of tests, we used an x-ray streak camera to obtain a continuous time resolution. The camera photocathode was about 7 m from the target, with the same 35° view as the diodes. In the sample data shown in Fig. 3, a short burst with a strong >5-keV x-ray emission is seen, followed by a series of weaker bursts. The streak image shows a more discrete structure than the corresponding PCD trace shown in Fig. 2. About one quarter of the width of the pulses in Fig. 3(a) is due to the streak response

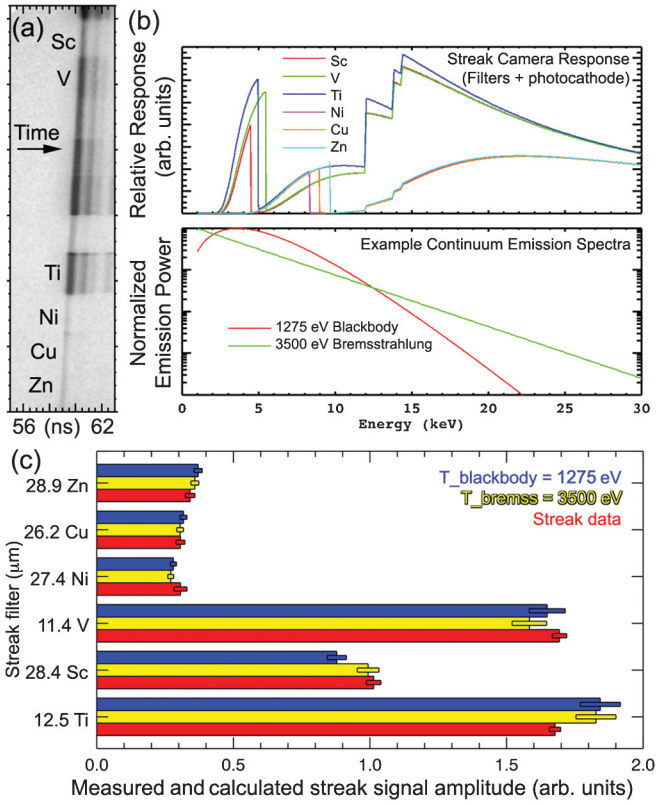

FIG. 3 (color). X-ray streak camera data from a W-Cu X-pinch test (s3859). (a) Time-calibrated streak image. The (slightly tilted) photocathode slit was covered with 12.7 μm Kapton (polyimide) and ten additional filters of different materials and thicknesses to provide spectral information. An additional 125 μm Kapton debris filter was also used. Accounting for the width of the static slit image, the data are consistent with a 0.4 ns main pulse duration. (b) Plot of the net streak camera response as a function of photon energy compared with two models for the continuum emission. (c) Comparison of measured and calculated signal amplitudes for six of the streak filters, using two different emission models. The data error bars represent film signal variations after background subtraction. The modeling error bars represent variations due to ±0.5 μm filter thickness uncertainties. Similar quality matches to the data are obtained for blackbody temperatures 1275 ± 75 eV and bremsstrahlung temperatures 3500 ± 500 eV.

(the static slit image is about 100 ps wide). Deconvolving this width from the data gives a full width at half-maximum for the >5-keV emission of about 0.4 ns. If the streak camera was out of focus (a recurring problem here), the duration could be shorter.

The relative streak camera response from 1–30 keV shown in Fig. 3(b) was determined using the transmission of the various filters [22] with a model for the back-surface quantum yield of the 102-Å Au photocathode [23]. The image in Fig. 3(a) was processed to find out the relative signal amplitudes for the first x-ray bursts through each of the six different filters [see Fig. 3(c)]. These data are compared with the blackbody and bremsstrahlung model results for the continuum radiation. Since the absolute response of the streak camera is unknown, the model results were normalized to match the total amplitude of the six data signals. Clearly, to distinguish between the two models, it would have been desirable to obtain data at the >10-keV level, but the streak camera did not have a sufficient dynamic range to permit this. A range of temperatures give similar fits to the data. Above and below this range, the relative amplitudes of the low- and high-energy filter groupings disagree with the data. The slope of the 5–10-keV continuum measured using a time-integrated spectrometer on the W and W-Cu experiments is also consistent with the slope implied by this time-resolved streak data. In Cu-Ni-Mn experiments, we observed strong K-shell radiation from Cu, Ni, and Mn, implying low-keV electron temperatures. Cu radiation was suppressed and the continuum stronger in W-Cu experiments, consistent with the higher efficacy of tungsten X pinches in converting electrical energy into radiation.

The source size in soft-x-rays was found using time-gated multilayer mirror (MLM) pinhole cameras [24]. Examples of monochromatic (277 eV) and broadband (> 1 keV) x-ray images are shown in Fig. 4. The 277-eV data are representative of the total soft-x-ray power data, and as in Fig. 4(a), this emission was always observed from a roughly 3-mm (or less) vertical region on solid-target X-pinch tests. The keV image was generally smaller, particularly during the first x-ray burst. In 0.2-MA experiments, the first x-ray burst is associated with the smallest x-ray source sizes, and later x-ray bursts are associated with subsequent disruption of the pinch plasma, as verified in radiography data [25]. We note that the best thermal radiation sources on SATURN are 20 mm–tall W-wire arrays that produce 75 ± 10 TW and 450 ± 50 kJ, for about 4 TW/mm and 23 kJ/mm [26]. The 10 TW and 165 ± 20 kJ made by our W X-pinch sources are comparable to the array results, being roughly 3 TW/mm and 55 kJ/mm. This is interesting, because unlike a cylindrical wire array, which involves a high-velocity implosion of mass to the array axis, all of the X-pinch mass starts on the axis, and the implosion kinetic energy remains low.

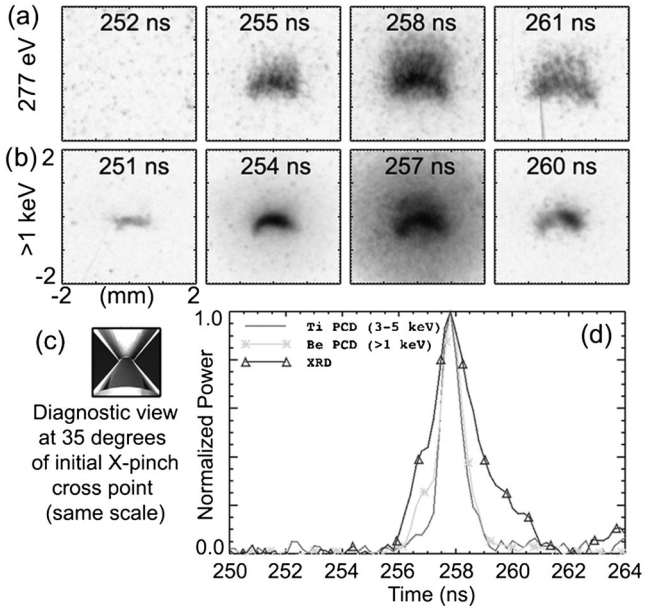

FIG. 4. Time-gated MLM pinhole camera images (4 mm by 4 mm, 3-ns gate times) from a Cu-Ni X-pinch test (s3812). (a) Monochromatic 277 eV image data (~ 0.5 mm resolution). (b) Broadband >1 keV image data (8-μm Be filter, ~0.2 mm resol.). (c) Solid model view of initial cross-point for comparison. (d) Plot of the soft x-ray diode and hard (PCD) x-ray power from the experiment. The cross-timing of each MLM row and each diode is accurate to ± 1.5 ns.

The time-integrated multi-keV source size was inferred with high spatial resolution using an array of 20-, 40-, and 80 μm wide slits at a distance of 100 mm, horizontally from the target and a detector at 660 mm. As was done previously [8,16], wave-optics modeling is used to calculate slit images for different source sizes. Only x-ray sources ≤ 9 μm in diameter project slit images with equal peak intensities at all the three slit sizes. For ≤ 3-μm sources, diffraction peaks become visible. Sample data consistent with a time-integrated 6–9 keV source size of 5-μm diameter are shown in Fig. 5. The slit measurements were very difficult to obtain because of the background from high-energy diffuse sources (e.g., post-pinch electron beams [27,28]), so only some tests succeeded in this direct measurement.

A key question is whether the bright spots in our 5-MA experiments correspond to more extreme states of matter than the observations from 0.2–1-MA experiments. We first note that the total 3–5-keV radiation power and energy from our 5-MA W X-pinch experiments are much higher than the ~2 J, 1–10 GW measured in 1-MA W X-pinch experiments [16] using the same techniques. Second, in some SATURN experiments, the same slits, filters, and similar films and magnification (about 6) were used as in our 1-MA experiments. The main difference was that the slits were located 1188 mm from the target instead of 137 mm, for a difference in solid angle of about 75.

Comparable film exposures were seen in both experiments for both Cu- and Ti-filtered slit images, showing a direct measurement that the bright spots are roughly ~75 times brighter.

Third, there is self-consistency in the measured radiation power, the measured source size, and the inferred blackbody spectrum, as may be implied from an analysis of Fig. 3. A 1275-eV (brightness temperature) blackbody emits 2.7×10^{21} W/m^2 in the 0.05–30 keV range. About 6×10^{20} W/m^2 of this passes through a 12.5-μm Ti filter, so that a Ti-filtered PCD would measure roughly 4.3 times less than the total radiated power from the blackbody. The assumption of a 1275-eV blackbody source implies that the ~90 GW measurements of Fig. 2(b) correspond to 0.4 TW of the total radiation of ~10 TW in Fig. 2(a), a reasonable fraction, with the remainder presumably coming from the larger surrounding plasma seen in Fig. 4. This assumption further implies a surface area of 1.4×10^{-10} m^2, corresponding to a 6.6-μm diameter for a spherical surface and consistent with the measurements in Fig. 5.

Finally, blackbody X-pinch sources are theoretically plausible. We ran three-dimensional radiation magnetohydrodynamic simulations of a tungsten X pinch on SATURN, using the GORGON code [13], with 1.6-μm resolution and random single-cell surface perturbations. As shown in Fig. 6, after an initial shock, a partly quasistatic compression phase follows, during which significant axial mass redistribution occurs and instabilities rapidly develop. As in 200-kA experiments [25], the necks "cascade", consistent with SATURN observations of both large, long-duration sources and multiple small bright spots. The radial compression is enabled in part by axial mass flow, but the cross-point region remains dense throughout the implosion. This simulation radiated about 4.5 TW at peak power in a near-blackbody spectrum, mainly from the narrow necks. The conditions at this time are extreme, with ~200-Gbar thermal pressures and magnetic pressures a few times that, for peak fields of about 150 000 T and peak densities >400 g/cm^3.

The calculated emission spectra, assuming a 6-μm diameter and 1.3-keV plasma, indicate that more than five times solid density would be required for the bright spot emission to be consistent with our streak data, peak radiated power, and time-integrated W-Cu spectra. For higher plasma temperatures of about 3 keV, near-solid densities would be consistent with our data. Densities that are 1–10 times solid are significantly higher than those inferred for lower-current bright spots, but they do not reach the extreme conditions predicted in Ref. [13].

Our data clearly show remarkable results from 5-MA X-pinch experiments, and clearly indicate that more extreme bright spot parameters such as power and brightness have been achieved than those from lower-current experiments. Without a better density measurement, it is difficult to conclude what the plasma pressure of our x-ray sources is. An alternative might be to measure the magnetic field associated with the extreme magnetic pressures predicted by simulations. At the ~100 000-T fields generated by MA

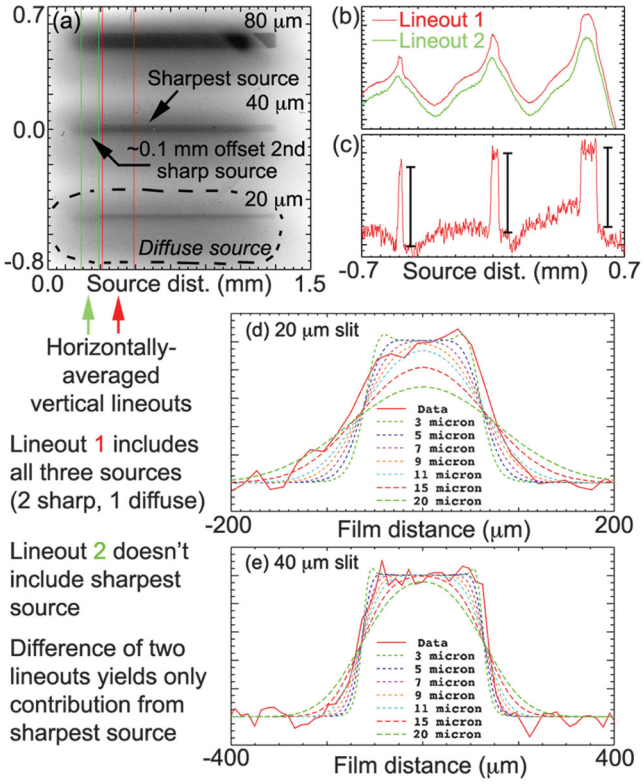

FIG. 5 (color). Time-integrated slit camera data (40 μm Cu filter) from a W X-pinch test (s3941). (a) A portion of the film image. Three offset x-ray sources produced sharp and diffuse projections of each of the 20, 40, and 80-μm slits. (b) Lineouts along the two regions from part (a). (c) The difference of the two lineouts from part (b). Vertical black bars of the same size are overlaid to illustrate that the three slit images have the same peak amplitude. (d) Simulated lineouts for a 20 μm slit calculated using wave-optics modeling assuming source sizes from 3 to 20 μm, overlaid with the normalized data from part (c). (e) The same for the 40 μm slit. The data are most consistent with a source size of 5 ± 2 μm.

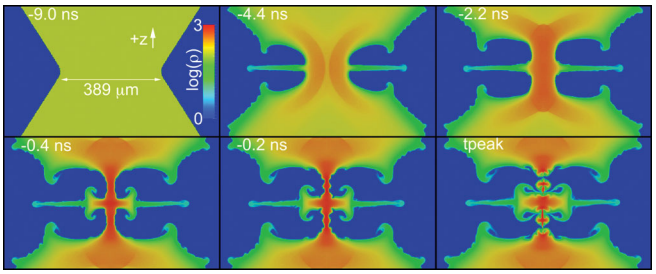

FIG. 6 (color). Log density (kg/m^3) slices through 3D magnetohydrodynamics simulations of a solid W X-pinch experiment. The times shown are relative to peak x-ray emission. The structure mostly remains cylindrically symmetric because of the large on-axis mass but the density and pressure at peak compression are limited by 3D asymmetry.

currents at ~3–5 μm diameters, Zeeman splitting of the order of tens of eV may be observable in x-ray emission lines, provided we could overcome density broadening [29]. We hope our data will help to motivate future experiments along these lines.

We thank Dr. Mark Herrmann for his encouragement, the SATURN operations crew for experimental support, Linda Nielsen for film support, and the Z load hardware team for hardware support. The project was funded in part by Sandia's Laboratory Directed Research and Development program. Sandia National Laboratories is a multiprogram laboratory managed and operated by Sandia Corporation, a wholly owned subsidiary of Lockheed Martin Corporation, for the U. S. Department of Energy's National Nuclear Security Administration under Contract No. DE-AC04-94AL85000.

[1] P. G. Burkhalter, C. M. Dozier, and D. J. Nagel, Phys. Rev. A **15**, 700 (1977).
[2] S. A. Pikuz, D. Sinars, T. Shelkovenko, K. Chandler, D. Hammer, G. Ivanenkov, W. Stepniewski, and I. Skobelev, Phys. Rev. Lett. **89**, 035003 (2002).
[3] K. N. Koshelev and N. R. Pereira, J. Appl. Phys. **69**, R21 (1991).
[4] B. A. Trubnikov, Fiz. Plazmy **12**, 468 (1986) [Sov. J. Plasma Phys. **12**, 271 (1986)].
[5] V. V. Vikhrev, Fiz. Plazmy **12**, 454 (1986) [Sov. J. Plasma Phys. **12**, 262 (1986)].
[6] N. R. Pereira and J. Davis, J. Appl. Phys. **64**, R1 (1988).
[7] S. M. Zakharov, G. V. Ivanenkov, A. A. Kolomenskii, S. A. Pikuz, A. I. Samokhin, and J. Ullschmeid, Pis'ma Zh. Tekh. Fiz. **6**, 1135 (1980) [Sov. Tech. Phys. Lett. **8**, 456 (1980)].
[8] B. M. Song, S. A. Pikuz, T. A. Shelkovenko, and D. A. Hammer, Appl. Opt. **44**, 2349 (2005).
[9] T. A. Shelkovenko, D. B. Sinars, S. A. Pikuz, K. M. Chandler, and D. A. Hammer, Rev. Sci. Instrum. **72**, 667 (2001).
[10] D. B. Sinars, S. A. Pikuz, T. A. Shelkovenko, K. M. Chandler, D. A. Hammer, and J. P. Apruzese, J. Quant. Spectrosc. Radiat. Transfer **78**, 61 (2003).
[11] S. B. Hansen, A. Shlyaptseva, S. Pikuz, T. Shelkovenko, D. Sinars, K. Chandler, and D. Hammer, Phys. Rev. E **70**, 026402 (2004).
[12] D. B. Sinars *et al.*, Phys. Rev. Lett. **100**, 145002 (2008).
[13] J. P. Chittenden, A. Ciardi, C. Jennings, S. Lebedev, D. Hammer, S. Pikuz, and T. Shelkovenko, Phys. Rev. Lett. **98**, 025003 (2007).
[14] S. S. Anan'ev *et al.*, JETP Lett. **87**, 364 (2008).
[15] S. S. Anan'ev *et al.*, Plasma Phys. Rep. **35**, 459 (2009).
[16] D. B. Sinars *et al.*, Phys. Plasmas **15**, 092703 (2008).
[17] T. A. Shelkovenko, S. A. Pikuz, R. D. McBride, P. F. Knapp, H. Wilhelm, D. A. Hammer, and D. B. Sinars, Phys. Plasmas **16**, 050702 (2009).
[18] T. A. Shelkovenko, S. A. Pikuz, A. D. Cahill, P. F. Knapp, D. A. Hammer, D. B. Sinars, I. N. Tilikin, and S. N. Mishin, Phys. Plasmas **17**, 112707 (2010).
[19] T. A. Shelkovenko, S. A. Pikuz, S. A. Mishin, A. R. Mingaleev, I. N. Tilikin, P. F. Knapp, A. D. Cahill, C. L. Hoyt, and D. A. Hammer, Plasma Phys. Rep. **38**, 359 (2012).
[20] D. D. Ryutov, M. S. Derzon, and M. K. Matzen, Rev. Mod. Phys. **72**, 167 (2000).
[21] T. C. Wagoner *et al.*, Phys. Rev. ST Accel. Beams **11**, 100401 (2008).
[22] B. L. Henke, E. M. Gullikson, and J. C. Davis, At. Data Nucl. Data Tables **54**, 181 (1993).
[23] B. L. Henke, J. P. Knauer, and K. Premaratne, J. Appl. Phys. **52**, 1509 (1981).
[24] B. Jones *et al.*, Rev. Sci. Instrum. **79**, 10E906 (2008).
[25] T. A. Shelkovenko, D. B. Sinars, S. A. Pikuz, and D. A. Hammer, Phys. Plasmas **8**, 1305 (2001).
[26] C. Deeney *et al.*, Phys. Rev. E **56**, 5945 (1997).
[27] V. L. Kantsyrev, D. A. Fedin, A. S. Shlyaptseva, S. Hansen, D. Chamberlain, and N. Ouart, Phys. Plasmas **10**, 2519 (2003).
[28] T. A. Shelkovenko *et al.*, Plasma Phys. Rep. **34**, 754 (2008).
[29] E. Stambulchik, K. Tsigutkin, and Y. Maron, Phys. Rev. Lett. **98**, 225001 (2007).